Mon. Not. R. Astron. Soc. **283,** L1–L5 (1996)

The nuclear torus in the active galaxy NGC 1068

S. Young, C. Packham, J. H. Hough and A. Efstathiou

Division of Physical Sciences, University of Hertfordshire, College Lane, Hatfield, Herts AL10 9AB

Accepted 1996 July 1. Received 1996 May 24; in original form 1996 February 21

ABSTRACT

We present near-infrared polarized images of the active galaxy NGC 1068. At these wavelengths, the counter-cone is observed in scattered light. At H (1.64 μm) we detect an absorption band across the counter-cone, which we interpret as absorption owing to the postulated torus. From a geometrical analysis we calculate that the torus is at a position angle of $32° \pm 3°$ on the plane of the sky, at an inclination to the line of sight (defined with respect to the polar axis) of $42° \pm 4°$, with a physical diameter greater than 200 pc. These figures are consistent with those derived from our models for the scattering of nuclear radiation and for the far-infrared emission from the torus.

Key words: polarization – scattering – galaxies: active – galaxies: individual: NGC 1068 – galaxies: Seyfert – infrared: galaxies.

1 INTRODUCTION

The unified theory of Seyfert active galaxies holds that the nuclei of both type 1 and type 2 objects harbour a featureless continuum source and a region of broad permitted emission lines (the broad-line region, or BLR), encircled by a geometrically and optically thick dusty torus. A region of narrow permitted and forbidden emission lines (the narrow line region, or NLR) extends along the poles of the torus. If the observer's line of sight to an object lies within the polar funnel of the torus then both emission line regions and the continuum source are observed and the object is classed as type 1. Otherwise, only the NLR is directly observed, resulting in a type 2 object. In the latter type of object, radiation from the continuum source and BLR, escaping out through the torus funnel, can be scattered into the line of sight, and the type 1 core can be detected in polarized flux. This was first demonstrated for the archetypal Seyfert 2 NGC 1068 (Antonucci & Miller 1985; Bailey et al. 1988).

The torus itself, although fundamental to the development of the unified theory, has not been directly observed. However, evidence for large amounts of dense gas at the centre of NGC 1068, which may be in the form of a torus, comes from CO observations (Planesas, Scoville & Myers 1991), which indicate a H_2 mass of $\sim 7 \times 10^8$ $M_\odot$ within 130 pc of the nuclear position. Also, observations of optically thick HCN emission, which requires large hydrogen column densities, imply an optical extinction in excess of 70 mag. In addition, these latter observations indicate a velocity gradient which, if arising from rotation, implies a rotation axis at a position angle of 33° on the sky, with a source size of ~180 pc (Jackson et al. 1993). Recent higher resolution HCN observations have confirmed these findings (Tacconi et al. 1994). Also, to account for the far-infrared emission observed in NGC 1068, a substantial amount of dust is required in a compact region (Pier & Krolik 1993; Efstathiou, Hough & Young 1995). Shadowing by the torus dictates that both the extended ionization by the continuum source and the scattering of nuclear radiation should occur in a bi-conical structure, and this has been observed for many active galaxies (Pogge 1988; Draper, Scarott & Tadhunter 1993; Wilson & Tsvetanov 1994). One of the cones will be on the far side of the host galaxy, and also on the far side of the active nucleus, and this implies that the torus should be detectable by its absorption of the scattered radiation from the far cone.

Here we present high spatial resolution near-infrared polarized images of NGC 1068 which show, for the first time, this absorption feature. Details of the observations and data reduction are contained in Section 2, and we describe the basic properties of the polarized images in Section 3. The results of the geometrical analysis are presented in Section 4, and we draw our conclusions in Section 5.

2 OBSERVATIONS AND DATA REDUCTION

The observations of NGC 1068 were obtained as part of the commissioning of the new dual-beam infrared polarimeter IRPOL2, built at the University of Hertfordshire, with the

near-infrared camera (IRCAM3) at the United Kingdom Infrared Telescope (UKIRT), Hawaii, on the nights of 1995 August 23 and 24. The camera uses a 256 × 256 InSb array with each pixel corresponding to 0.1286 arcsec on the sky. On-object exposures of 960, 720 and 640 s were made at *J* (1.23 μm), *H* (1.64 μm) and *K* (2.2 μm) respectively. Observations of blank sky were interposed with the object observations, and were used for sky subtraction. Observations of the twilight sky were used as a flat-field. Images taken with the polarimeter achromatic half-wave retarder at 0°, 45°, 22°.5 and 67°.5 were dark-subtracted, and cleaned of bad and hot pixels before being registered at the peak of emission and shifted. The polarization images were then formed using the Starlink Time-Series Polarimetry (TSP) package IRISPOL (Bailey 1993). The polarizing efficiency at each wavelength was checked by observing stars with a wire-grid of known polarization efficiency, and the absolute position angle of polarization was determined from measurements of polarized standards. The resulting data were then co-added at each wavelength and flux-calibrated from observations of stars from the UKIRT faint standard set (Casali & Hawarden 1993). Several of the observation sets were affected by telescope oscillations in right ascension, affecting both the apparent shape of the flux distribution and the measured polarization. The seeing was measured to be ∼ arcsec, with the oscillation extending this to 1.5 arcsec in RA. This effect was minimized using the Starlink CCDPAK routine TRANNDF, the results of which were checked against those observations not greatly affected by the oscillation and were found to be in excellent agreement.

3 THE POLARIZED IMAGES OF NGC 1068

The *H*-band polarization vector map from the total data set is displayed in Fig. 1, superimposed on the total flux contours, with north to the top and east to the left. Clearly visible to the north-east of the nucleus is the part-centrosymmetric pattern of polarization vectors associated with the scattering cone detected at optical wavelengths (Miller, Goodrich & Mathews 1991; Scarrott et al. 1991). Also seen at these near-infrared wavelengths is a similar pattern of polarization vectors to the south-west, indicative of scattering of nuclear radiation in a counter-cone. On Fig. 2 we present a polarized intensity image of NGC 1068 from the same *H*-band data set. Both the forward cone and the conter-cone are, again, clearly visible, along with a 'knot' of polarized light ∼4.5 arcsec to the north-east of the nucleus, first observed at optical wavelengths (Miller et al. 1991; Scarrott et al. 1991). At optical wavelengths the counter-cone is not visible, indicating that the scattered radiation undergoes significant extinction which implies that the counter-cone is on the far side of the host galaxy and viewed through the dusty disc of the host galaxy. Since NGC 1068 is at the low inclination of ∼20° to the plane of the sky (Baldwin, Wilson & Whittle 1987; Scoville et al. 1988), this also implies that the counter-cone is directed away from us. It should also be noted that the counter-cone appears to be brighter than the forward cone in polarized flux. The simplest explanation is that the number density of scatterers is greater in the counter-cone than in the forward cone, and hence a greater proportion of the nuclear radiation is scat-

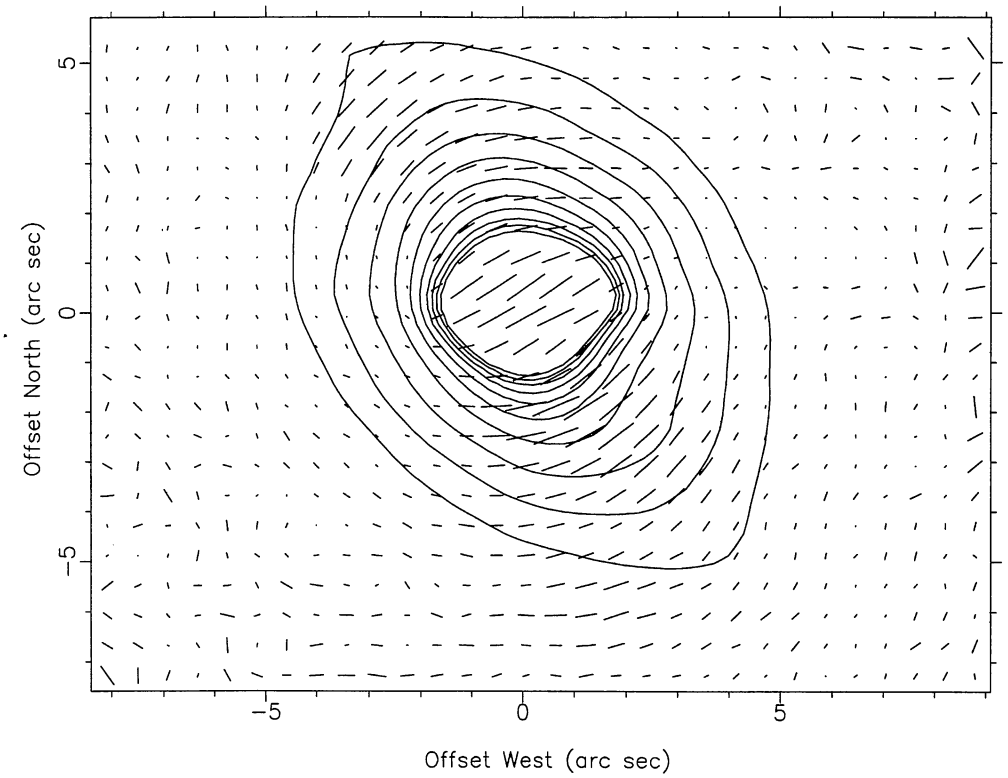

Figure 1. The polarization vectors in the *H* band (1.64 μm), superimposed upon the total intensity contours for the image of the combined data set. The image is approximately 17 × 13 arcsec^2 and the pixels are 0.286 arcsec square. The length of a 100 per cent polarization vector would be 5.72 arcsec.

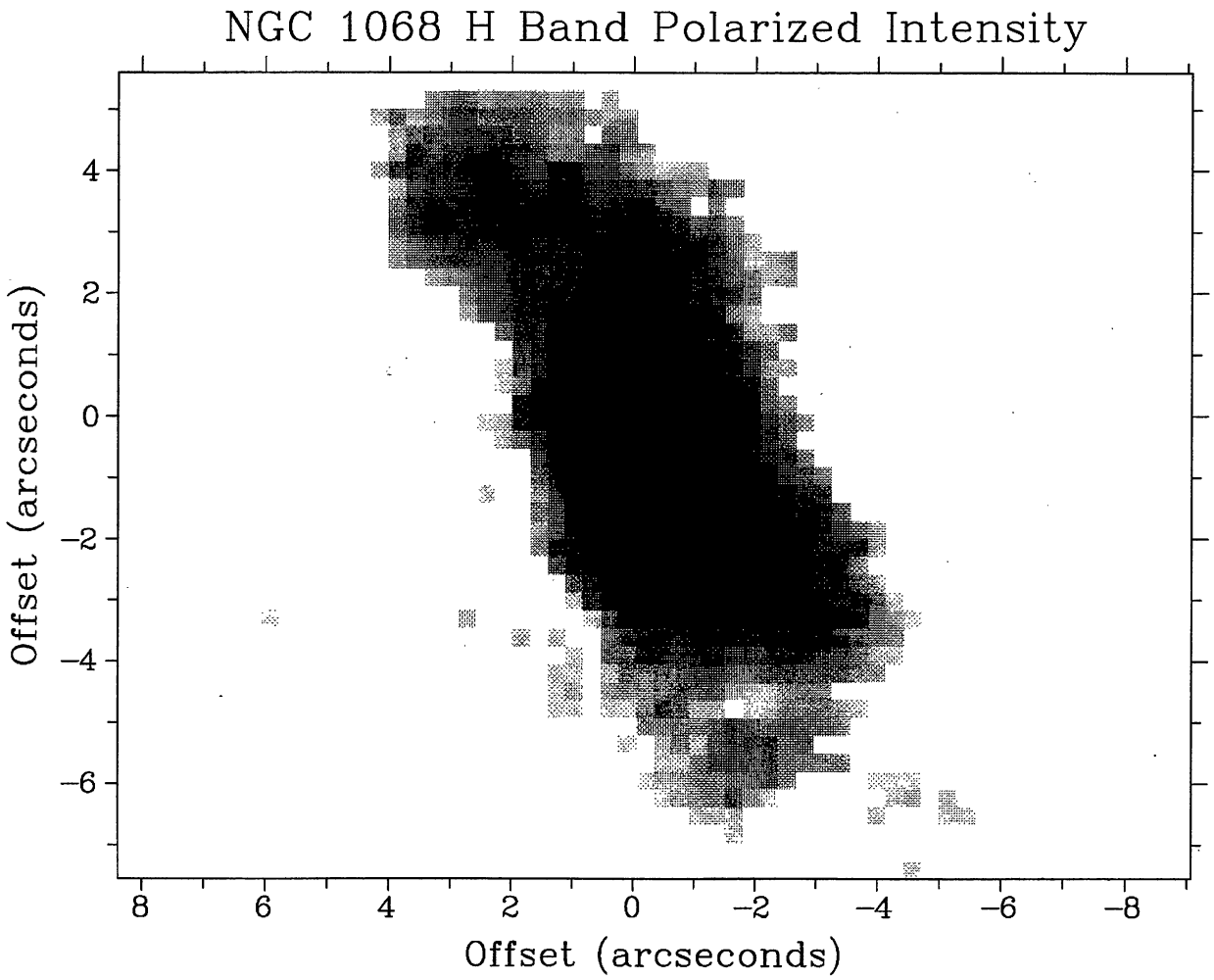

Figure 2. A grey-scale polarized flux image of NGC 1068 in the *H* band (1.64 μm).

tered. There is no a priori reason why the two cones should have the same number density of scatterers.

Since the counter-cone is pointing away from us, it must also lie behind part of the torus, and scattered radiation from this part of the cone will be blocked by the torus, which is optically thick even at these wavelengths. The torus should, therefore, be visible as an absorption band against the counter-cone. Fig. 2, the *H*-band polarized flux image, shows this to be the case. A cut along position angle (PA) 32° is shown in Fig. 3 (positive numbers on the arcsec axis indicating a north-easterly direction on the sky), which clearly shows the absorption trough associated with the torus at a distance of ~1.2 arcsec from the peak of polarized flux. Seeing and the RA oscillation mean that light from the bright regions partially fills in the absorption band. The error bars shown in Fig. 3 are the standard deviation derived from the spread of the individual polarized flux images.

An alternative explanation for the band across the counter-cone is that it is simply a region devoid of scatterers. Examination of the *K*-band image (Fig. 4) shows that this is not the case. The most obvious difference from the *H*-band image is that the dark band just south of the nucleus is not present, and we also note that the polarized flux is more centrally peaked. This can be explained in terms of our model for the polarization properties of NGC 1068 (Young et al. 1995), where the optical polarization is due to electron scattering but a dichroic view of the near-infrared-emitting region, through the torus, becomes more important at longer wavelengths. At *K*, this dichroic polarization dominates the integrated polarized flux, and, since it lies through the torus, the absorption band is less distinct. Even if this model is not correct, the fact that the band is filled in at *K* shows that there is absorption of the scattered radiation, and thus the H-band image is not a result of two scattering regions. However, our model is supported by the difference in the centroid of the total flux from that of the polarized flux. This is greatest at *J*, where most of the polarized flux is from scattering, the scattering region not being exactly at the nucleus, and zero at *K* where the dichroic absorption of the nuclear radiation dominates.

The *J*-band image is very similar to the *H*-band image and

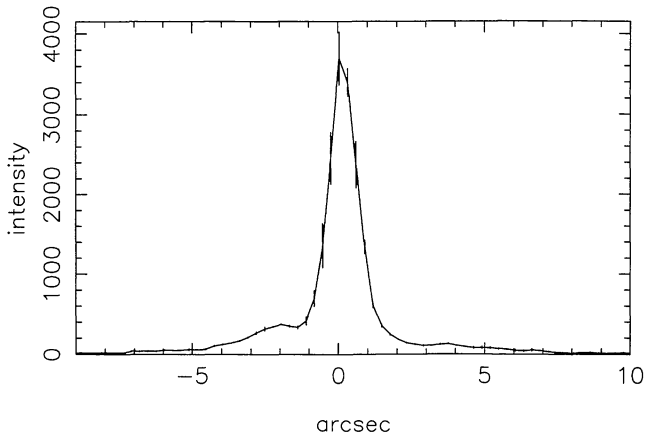

Figure 3. An intensity cut along a position angle of 32° (east of north) through the calculated position of the active nucleus (at 0 arcsec; negative arcseconds indicate a south-westerly direction, and positive arcseconds indicate positions north-east of the nucleus).

has not been shown.

4 DERIVED PARAMETERS FOR THE TORUS OF NGC 1068

Assuming that the torus is circular, it should be possible to determine its size, inclination to the line of sight and position angle on the sky. However, knowledge of the true nuclear position is also required, and this has been obtained by three independent methods for both the *J*- and *H*-band images. First, in the *J*-band, unpolarized stars are dominant (Young et al. 1995), and the flux from these should peak at the true nuclear position. However, it should be noted that the peak of flux in the optical is not at the nuclear position (Evans et al. 1991; Caganoff et al. 1991). At *H*, the peak in polarized flux is primarily due to the dichroic view of the nucleus, thus revealing its position. The second method of determining the nuclear position is to trace back the normals to the position angle of polarization in the scattering region, as successfully demonstrated at ultraviolet wavelengths (Axon et al. 1995). Thirdly, the edges of the cones can be traced back to the nucleus. All three methods produced consistent results, the dispersion between them indicating that the nucleus has been located to an accuracy of 0.15 arcsec. This position has been used for the zero of coordinates in all the figures.

We have fitted ellipses to the torus absorption in polarized flux, centred on the derived nuclear position. Assuming a distance to NGC 1068 of 14.8 Mpc (Tully 1988), giving a spatial scale of 71 pc arcsec^{-1}, we derive a PA on the sky for the torus of $32° \pm 3°$, an inclination to the line of sight of $42° \pm 4°$, and a torus diameter greater than 200 pc. Only a lower limit for the torus size can be calculated because of the effects of seeing. The values derived from the *J*-band image were within these errors.

The calculated PA and inclination are entirely consistent with previously derived values. An inclination of $\sim 35°$ is calculated from models of the scattered nuclear radiation (Miller et al. 1991; Young et al. 1995), and a value of $\sim 45°$

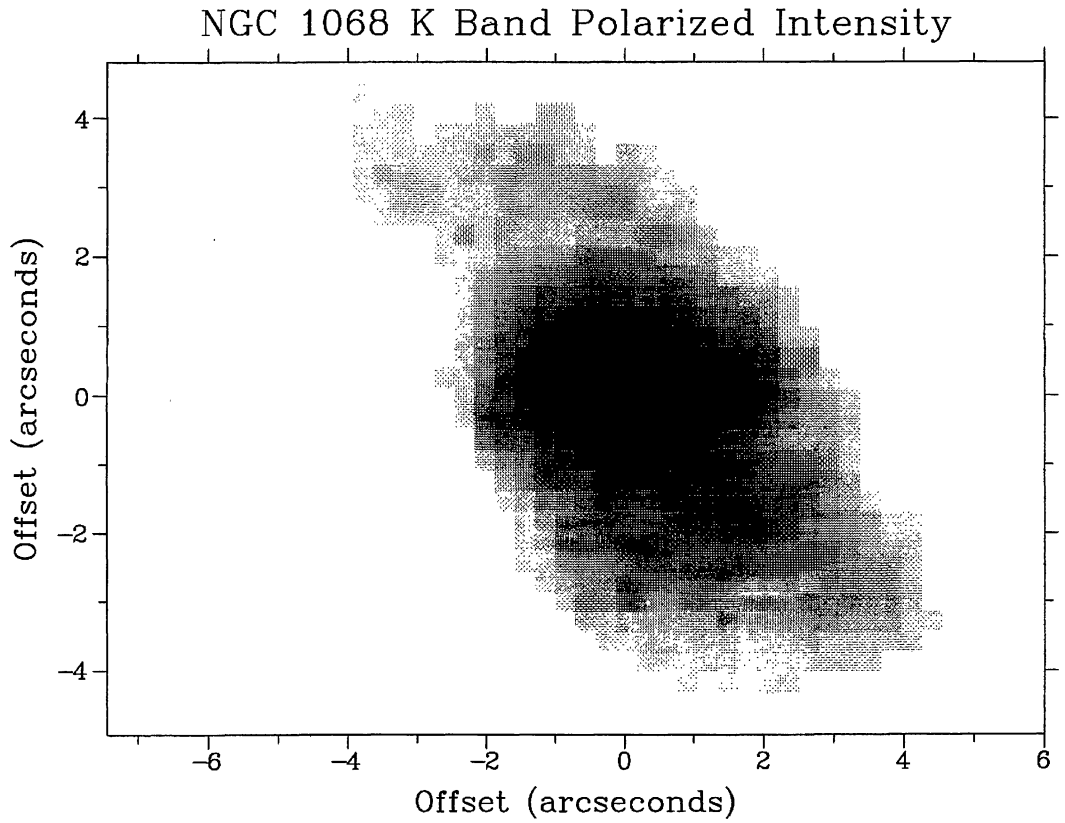

Figure 4. As for Fig. 2 but in the *K* band (2.2 μm).

is obtained from modelling of the infrared emission of the torus (Efstathiou et al. 1995). The PA on the sky has been estimated as $32° \pm 5°$ from the axis of the emission-line cones (Pogge 1998) and the large-scale radio structures (Wilson & Ulvestad 1983, 1987). The size of the torus is consistent with the value of 178 pc derived from our infrared emission models of the torus (Efstathiou et al. 1995). The estimated size and inclination are not consistent with models of the infrared emission that favour very compact tori (Pier & Krolik 1993). The very fact that a counter-cone is observed is also evidence against the warped disc model (Phinney 1989), in which an optically thick, kiloparsec-scale structure is envisioned. The calculated values for the size and inclination of the torus compare favourably to those derived for the gaseous disc responsible for the HCN emission (Jackson et al. 1993; Tacconi et al. 1994).

The torus size is similar to that of the dusty disc or torus observed in total flux for the radio-loud galaxy NGC 4261 (Jaffe et al. 1993) with the *Hubble Space Telescope*. If the host galaxy of NGC 4261 contains only small amounts of dust, then stars can be observed throughout the body of the galaxy. Some of the stars will be on the far side of the torus and their radiation will be obscured by it, allowing the torus to be 'seen'. For NGC 1068 the dusty disc of the host spiral galaxy, which obscures the counter-cone from view at optical wavelengths, will also attenuate the light from the stars on the far side of the galaxy, and thus near-side stars will dominate. The torus sits behind these stars and thus cannot have any observable effect on their radiation. The torus is therefore best viewed in polarized flux, where the counter-cone provides the background illumination.

5 CONCLUSIONS

We have presented evidence showing that the torus in NGC 1068 is at an inclination of $42° \pm 4°$, similar to that expected from models of the polarization characteristics from the ultraviolet to the near-infrared, and at a position angle on the sky of $32° \pm 3°$, the same as that suggested by the rotation measured from the optically thick HCN observations and the position angle of the large-scale radio and ionization structure in NGC 1068 (Wilson & Ulvestad 1983, 1987). We also show that the torus has a size of the order of 200 pc. This is substantially larger than has been predicted, but is consistent with our recent models for the far-infrared emission from the torus, and the size of the region from which molecular emission is observed, and similar to the disc size required to explain the differences between type 1, type 2 and intermediate Seyferts (Maiolino et al. 1995; Maiolino & Rieke 1995).

ACKNOWLEDGMENTS

We thank Colin Aspin and the other staff at UKIRT for their support, Tim Gledhill for his help with the observations, Neasa Foley for the instrument control software, and the staff in the workshops of the University of Hertfordshire's Division of Mechanical & Aeronautical Engineering and Physical Sciences, for their help in building IRPOL2.

REFERENCES

Antonucci R. R. J., Miller J. S., 1985, ApJ, 297, 621
Axon D. J., Capetti A., Macchetto F., Sparks W. B., Boksenberg A., 1995, in Ward M. J., ed., Proc. Oxford Torus Workshop. Oxford University, p. 25
Bailey J. A., 1993, Starlink User Note 66.2: TSP Version 2.1
Bailey J., Axon D. J., Hough J. H., Ward M. J., McLean I., Heathcotte S. R., 1988, MNRAS, 234, 899
Baldwin J. A., Wilson A. S., Whittle M., 1987, ApJ, 319, 84
Caganoff S. et al., 1991, ApJ, 277, L9
Casali M., Hawarden T., 1993, JCMT–UKIRT Newsletter, 4, 33
Draper P. W., Scarrott S. M., Tadhunter C. N., 1993, MNRAS, 262, 1029
Efstathiou A., Hough J. H., Young S., 1995, MNRAS, 277, 1134
Evans I. N., Ford H. C., Kinney A. L., Antonucci R. R. J., Armus L., Caganoff S., 1991, ApJ, 369, L27
Jackson J. M., Pagalione T. A. D., Ishizuki S., Nguyen-Q-Rieu, 1993, ApJ, 418, L13
Jaffe W., Ford H. C., Ferrarese L., van den Bosch F., O'Connell R. W., 1993, Nat, 364, 213
Maiolino R., Rieke G. H., 1995, ApJ, 454, 95
Maiolino R., Ruiz M., Rieke G. H., Keller L. D., 1995, ApJ, 446, 561
Miller J. S., Goodrich R. W., Mathews W. G., 1991, ApJ, 378, 47
Phinney E. S., 1989, in Meyer F., Dischl W. J., Frank J., Meyer-Hofmeister E., eds, Theory of Accretion Disks. Kluwer, Dordrecht, p. 457
Pier W. A., Krolik J. H., 1993, ApJ, 418, 673
Planesas P., Scoville N. Z., Myers S. T., 1991, ApJ, 369, 364
Pogge R., 1988, ApJ, 328, 519
Scarrott S. M., Rolph C. D., Tadhunter C. N., Wolstencroft R. D., 1991, MNRAS, 249, 16P
Scoville N. Z., Mathews K., Carico D. O., Sanders D. B., 1988, ApJ, 327, L61
Tacconi L. J., Genzel R., Bleitz M., Cameron M., Harris A. I., Madden S., 1994, ApJ, 426, L27
Tully R. B., 1988, Nearby Galaxies Catalog. Cambridge Univ. Press, New York
Wilson A. S., Tsvetanov Z. I., 1994, AJ, 107, 1227
Wilson A. S., Ulvestad J. S., 1983, ApJ, 275, 8
Wilson A. S., Ulvestad J. S., 1987, ApJ, 319, 105
Young S., Hough J. H., Axon D. J., Bailey J. A., Ward M. J., 1995, MNRAS, 272, 513